ORIGINAL PAPER

3D Extrusion Printability of Rice Starch and Optimization of Process Variables

Radhika Theagarajan[1,2] · J. A. Moses[1] · C. Anandharamakrishnan[1] ⓘ

Abstract

Three-dimensional extrusion printing is an additive manufacturing approach with numerous emerging applications in the food industry. In this research, the effect of nozzle size (1.2 to 1.7 mm), print speed (800 to 2200 mm/min), and motor speed (120 to 240 rpm) on the printability of rice starch were studied. Uniformity and ease of extrusion were considered, and the printed constructs were carefully observed for thread quality, binding property, finishing, texture, layer definition, shape, dimensional stability, and appearance. The rheological behavior of the material supply was studied, and the scientific rationale behind the printability of starch is discussed in detail. Printing rice starch at higher motor speeds (180–240 rpm) with lower printing speeds (800–1500 mm/min) resulted in better printability. The results of this study would be a foundation for future 3D food printing studies using rice starch.

Keywords 3D food printing · Printing behavior · Rice starch · Rheology · Additive manufacturing

Introduction

3D printing is an emerging concept in the food industry, allowing the development of complex geometric shapes made out of food ingredients. Importantly, 3D printing can allow excellent levels of customization in terms of shape and in personalized delivery of nutrients (Kumar et al. 2020). With several other advantages, 3D printing has enormous prospects of globalization (Nachal et al. 2019). Among various food printing techniques, extrusion-based 3D printing involves the pressure-driven extrusion of a semi-solid material supply through a nozzle for layer-by-layer fabrication of 3D structures (Nida et al. 2020). Extrusion printing includes both hot and cold extrusion methods. Hot melt extrusion printing can convert raw food ingredients such as chocolates to ready-to-serve end products (Chen et al. 2019). Almost all cold extruded 3D printed constructs require an additional post-processing operation. Food matrices are complex, and all food components are not natively printable; several food material supplies require to be pre-processed in order to make them printable. This can be done with the addition of additives such as hydrocolloids that can alter the material's viscosity by the formation of gel networks (Prabhuswamy et al. 2019) or through one of the several unit operations that can change the functionality of the material supply (for example, by gelatinization).

In this research, rice starch was used as the printing material supply. Rice starch in the form of rice flour is widely used as a key ingredient in developing several indigenous food products (Prabhakaran and Moses 2016). This in turn relates to the composition and structure of rice starch, and these are highly dependent on the rice variety apart from several other factors (Saikrishna et al. 2018). The endosperm of rice is valued for its high protein digestibility, and rice starch is non-allergic (Shahzad et al. 2019). Rheology and extrudability of the starch can be linked with the interaction of starch and water, amylose content, amylose:amylopectin ratio, granule size, and degree of polymerization. Importantly, starch lipids are unique to cereal endosperms (Gayral et al. 2018). These can serve as the functional component responsible for the extrudability of starch.

Though the extrudability of rice starch has been reported by previous researchers, an in-depth understanding of its printability can provide valuable insights for future 3D printing

✉ C. Anandharamakrishnan
anandharamakrishnan@iifpt.edu.in

1 Computational Modeling and Nanoscale Processing Unit, Indian Institute of Food Processing Technology (IIFPT), Thanjavur, India

2 Bharathidasan Univeristy, Tiruchirappalli, Tamil Nadu, India

applications involving rice starch or its combination with other ingredients. Starches have been used widely in a range of 3D food printing applications (Sun et al. 2015; Dong et al. 2019; Chuanxing et al. 2018). In a recent study, rice flour was added at various levels to improve the printability of egg white and egg yolk (Anukiruthika et al. 2020). In another study, the printability of brown rice was studied and improved with the addition of hydrocolloids (xanthan gum and guar gum) (Huang et al. 2019). In this study, white rice starch was printed as such, without any additives; the effect of varying printing conditions on its extrusion printability was studied. Studies explain that higher concentrations of starch can perform the role of hydrocolloids (Tan et al. 2018). This links to the rationale that the addition of water to starch molecules results in the formation of continuous matrices of interwoven amylose molecules and swollen granules (Chen et al. 2019), therefore improving printability. Considering these aspects, the objective of this research was to provide an in-depth understanding on the printability of rice starch and to optimize its 3D extrusion printing conditions.

Materials and Methods

Extraction of Rice Starch

Rice kernels (var. *Ponni*) were procured from the local market at Thanjavur, India. Satake rice milling machine (Satake Engineering Co., India) was used to mill the kernels, and the rice flour was assessed for physical impurities. The extraction of starch was performed by the wet extraction method adopted by Daiuto et al. (2005) with some modifications. Rice flour was suspended in distilled water (at 1:10 w/v). The suspension was mixed well and filtered using a double-fold muslin cloth. The filtrate was left undisturbed overnight in a refrigerator so that the starch settles down. The supernatant was discarded, and the residue was oven-dried at 50 °C and stored under ambient conditions for further analyses.

Characteristics of Raw Material

Particle Size Distribution

Moisture-free samples were subjected to sieve analysis to determine the average particle size according to ASABE Standard S319.4 (ASABE Standards 2008). The sample (100 g) was loaded on the top-most sieve of a collection of sieves arranged in their order of decreasing apertures in a gyratory sieve shaker (Ro-Tap). The sieves were numbered, and the empty weight of each sieve was noted before the sieve analysis. After the sieving process, the mass of the sample

retained on each sieve was noted. The geometric mean diameter of rice starch powder was calculated using Eq. 1.

$$d_{\mathrm{gw}} = \log^{-1} \frac{\sum_{i=l}^{n} \left(W_i \log \overline{d_i} \right)}{\sum_{i=1}^{n} W_i} \qquad (1)$$

where, d_{gw} is the geometric mean diameter of the particles (mm), d_i is the nominal sieve aperture size of the ith sieve (mm), and W_i is the mass on the ith sieve (g). Morphology and particle size have significant effects on the functional properties of the starch (Bhat and Riar 2019).

Composition of Rice Starch

The proximate composition of rice starch was estimated by the methods adapted by Horwitz and Latimer (2000). The method described by Juliano (1971) was adapted for the estimation of amylose content in the rice starch. The amylose content was expressed as a percentage against the total sample taken for estimation on dry basis weight (Riaz et al. 2018).

Water Absorption Capacity

The water absorption capacity of rice starch was determined using the method described by Sosulski et al. (1976). Briefly, 1 g of sample was mixed thoroughly with 10-ml distilled water, and the mixture was allowed to stand at ambient temperature (30 ± 2 °C) for 30 min, and then centrifuged for 30 min at 3000 rpm.

Bulk Density, True Density, and Void Fraction

Bulk density (ρ_b) of rice starch powder was estimated according to the method described by Okaka and Potter (1977) by filling 10 g of the sample in a 30-ml graduated cylinder with gentle tapping of the cylinder, eight to ten times. The final volume of the sample was measured and expressed in g/ml (Eq. 2).

$$\text{Bulk density} \left(\frac{\text{g}}{\text{ml}} \right) = \frac{\text{Weight of the sample}}{\text{Volume occupied by the sample}} \qquad (2)$$

True density (ρ_t), defined as the ratio between the mass of the sample and the true volume of the sample was determined by the toluene displacement method (Okaka and Potter 1977). Void fraction (ε) that explains the ratio of inter-granular space to the total space occupied by the starch was computed using Eq. 3. Understanding the void fraction can be useful in explaining the extrusion pattern of rice starch packed as a dough system.

$$\text{Void fraction } \varepsilon = \frac{\rho t - \rho b}{\rho t} \times 100 \qquad (3)$$

Color Analysis

The color of rice starch and the material supply were analyzed using in a Hunter Lab colorimeter (Model, Labscan XE, USA) as $L*$, $a*$, and $b*$ values. The $L*$ value corresponds to the level of lightness or whiteness, $a*$ value specifies redness or greenness, and $b*$ value denotes the yellowness to blueness of the sample. Before analysis, the instrument was calibrated with standard white and black tiles.

Pasting Behavior

Pasting properties of rice starch sample were determined using a rheometer (MCR-52, Anton Paar GmbH, Germany). Maximum, minimum, and final viscosities, breakdown, and consistency were read automatically from the in-built software. Rheology of rice starch was performed according to the method described by Wang et al. (2002). The rice starch (3.3 g) was mixed with 25-ml distilled water, and the slurry was subjected to a temperature rise from 50 to 95 °C. Rise and fall in temperature can result in structural deformation of starch granules and gel formation effects (Cameron et al. 2007).

Characteristics of the Material Supply Used for 3D Printing

Rice starch was mixed thoroughly with an equal amount of water to prepare the dough-like material supply. Understanding the properties of the material supply is essential as it can be directly linked with its printability and post-processing characteristics.

Water Activity

Water activity (a_{w}) of the rice starch paste was determined using a water activity meter (AQUALAB 4TE, USA) at 25 ± 1 °C. Generally, products with lesser a_{w} can provide better storage stability (Theagarajan et al. 2019).

Rheological Behavior

Rice paste behaves as a non-Newtonian fluid, with viscosity dependent on the applied shear. It is essential to relate the rheological properties of the rice paste with the consistency required for printing and the post-printing mechanical stability of the 3D constructs. Understanding the rheology of starch can explain how its properties change upon interaction with water, also providing insights on its state of dispersions, emulsions, and gels. Also, it is important to know the flow behavior, and further investigation can explain the effect of process variables on the material (Li and Nie 2015). Importantly, rheological behavior is crucial in the context of extrusion-based 3D food printing.

Steady Shear Rate

The relationship between apparent viscosity and the shear rate was obtained by studying the flow behavior of the rice starch using a rheometer (MCR-52, Anton Paar GmbH, Germany) with parallel plate geometry with a diameter of 20 mm. Around a 1-mm gap was set, and the analyses were carried out at 25 °C. After the sample was loaded, the geometry was set at its measuring position; the excess sample was trimmed out from edges (Liu et al. 2019b). The obtained rheological values were fitted to the power law model to explain the relationship between apparent viscosity and shear rate (Eq. 4).

$$\tau = k\gamma^n \tag{4}$$

where τ is the shear stress (Pa), k is the flow consistency index (Pa.s^n), γ is the shear rate (s^{-1}), and n is the flow behavior index.

Oscillatory Viscosity

Viscoelastic property of the rice starch dough was analyzed with a rheometer (MCR 102 series, Anton Paar Co. Ltd., Austria). Parallel plates with a diameter of 50 mm and a gap distance of 2 mm were used for the analysis. Measurements were carried out at 25 °C. Frequency sweep was conducted from 0.1–500 rad/s, considering the linear viscoelastic region of rice starch. Temperature sweep was carried out at 40 to 100 °C. Storage modulus (G'), loss modulus (G"), and loss tangent were analyzed. Storage modulus (G') is a measure of the elastic gel–like behavior of the material, indicating that the samples are resistant towards the elastic deformation, while loss modulus (G") represents the viscous response of the material. The loss tangent (tan δ = G"/G') is used to determine the viscoelastic behavior of a sample. Samples with tan δ value lesser than one exhibit elastic properties, and those with tan δ greater than one show viscous property (Yang et al. 2018).

The Printing Process

The in-house developed extrusion-based delta model 3D printer CARK (Controlled Additive Manufacturing Robotic Kit) reported by Anukiruthika et al. (2020) and Keerthana et al. (2020) was used for the study (Fig. 1). The printing was performed through extrusion supported by a controlled air pressure system that could operate up to 4 bar. XYZ directional movements (using delta arms) were controlled with Simplify3D (Simplify3D®, Cincinnati, OH). The design to be printed, available as a stereolithography file, was sliced into G-codes. A stepper motor system supported the printer and was software-controlled and synchronized with the printer. The motor was directly connected to the auger drive set (extruder assembly), and this set up helped in the extrusion process. The 30 cm^3 syringe barrel was filled with the rice starch

Fig. 1 Schematic representation of the 3D printer CARK used in this study (Source: Anukiruthika et al. 2020)
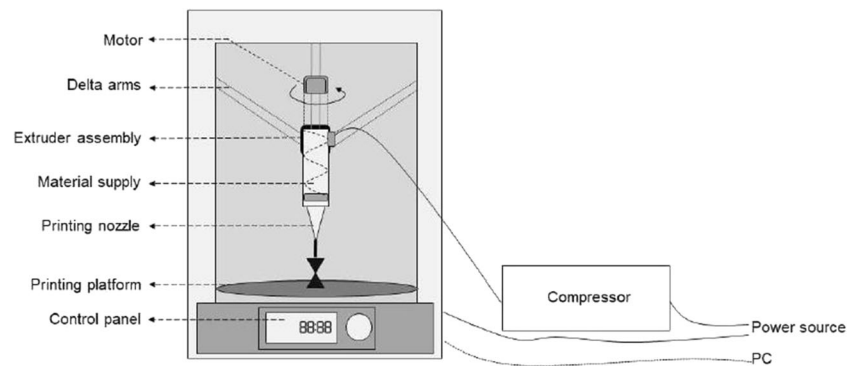
material supply for all 3D printing trials. Cube shape was printed using the 3D printer at room temperature. Based on preliminary trials, 4 bar pressure was kept constant throughout the study. Infill percentage affects the stability of the 3D construct and was kept constant (100%) for all printing trials. All 3D printed constructs were deposited over a flat printing platform.

Printing Rate

The printing rate (g/s) was determined using the method followed by Mantihal et al. (2017). It was obtained by dividing the weight of the printed product by the total time required to print the sample.

Evaluation of 3D Printed Rice Starch

Microscopic Analysis

The microstructure of the printed constructs was evaluated using a stereomicroscope (Motic* K Series Sterio, Model K-400 L Leica Microsystems Ltd., Wetzlar, Germany) (Samli et al. 2013). Structural construction and layer deformity were observed. At 20X magnification, images were captured and recorded using Leica S8APO - DFC295 software.

Texture Analysis

Textural characteristics of 3D printed rice starch were determined in terms of hardness, fracturability, adhesiveness, and springiness using a Texture Analyser (TA-XT2i; Stable Microsystems, UK). A cylinder probe (P/5) was used for the study. These parameters were then used to explain the strength of the printed 3D constructs (Dong et al. 2019).

Sensory Evaluation

Visual perception of 3D printed rice starch was analyzed by a 20-membered semi-trained panel who graded the constructs on a nine-point hedonic scale (Ghazal et al. 2019). Sensory parameters like appearance, dimensional stability, shape, layer definitions, texture and finishing, binding property, and thread quality were observed. These observations showed a significant relationship with printing conditions.

Assessment of Printing Behavior

With the optimized parameters, during the printing process, the shear rate, and extrusion rate of the rice starch material supply were evaluated. The shear rate exerted during the extrusion process was calculated using (Eq. 5) (Le Tohic et al. 2017).

$$\gamma = \frac{8v}{d} \tag{5}$$

where γ is the shear rate (s^{-1}), d is the diameter of the nozzle (mm),

$$v = Q/A \tag{6}$$

where v is the average velocity (mm s^{-1}), Q is the extrusion rate (mm^3 s^{-1}), and A is the cross-sectional area of the nozzle (mm^2).

Statistical Analyses

All experiments were conducted thrice, and data are expressed as mean and standard deviation (SD) of the three independent experiments. One-way ANOVA was conducted on the mean values to assess significant differences in the data at $p \leq 0.05$ using SPSS software (version 20; IBM Inc., Armonk, NY, USA).

Results and Discussion

Characterization of the Raw Material

Particle Size Distribution

Based on experimental values, the particle size distribution curve for rice starch was plotted (Fig. 2). The average particle

size was calculated to be 0.31 mm. From this data, the modulus of fineness can be determined (Alex et al. 2016). Particle size can greatly influence the printing precision and resolution of 3D printed constructs (Godoi et al. 2016). In addition, the particle size of the starch greatly influences its pasting properties (Asmeda et al. 2016). It has implications on the physicochemical properties of flours, and changes in surface area per unit volume can be linked to the bioavailability of macronutrients (De La Hera et al. 2013). In case of certain food constituents such as fiber, improper control over particle size can be associated with nozzle-clogging.

Composition of Rice Starch

The moisture content of the rice starch was found to be $7.4 \pm 0.51\%$ d.b. Moisture content has implications on the printability, and the moisture content of the printed and post-processed product is a crucial parameter for storage stability. The rice starch contained 85.04 ± 1.54 carbohydrate, 0.66 ± 0.05 fat, 5.73 ± 1.10 protein, 0.6 ± 0.05 crude fiber, and 0.43 ± 0.04 ash (all values are in g/100 g), with an energy value of 369.77 ± 2.32 kcal.

Amylose Content

The amylose content of starch can be an index to explain the properties of the starch and its applications. The rice starch used for the 3D printing material supply was extracted from medium amylose rice, with amylose and amylopectin contents estimated to be $20.03 \pm 0.3\%$ and $79.96 \pm 0.3\%$, respectively. The physicochemical properties of rice starch are largely dependent on these starch fractions. For example, variations in amylose content will have implications on the product texture; lower amylose content would result in cohesiveness,

tenderness, and smoothness, adversely affecting stability of printed structure. Moreover, there is an improvement in the shear thinning behavior with an increase in amylose content; this is due to an increase in entanglements between the amylose chains (Román et al. 2018). High amylose content starch absorbs more water, and the water holding capacity is critical in case of extrusion-based 3D printing material supplies (Cao et al. 2020; Riaz et al. 2018; Shen et al. 2019). The significance of amylose content in the printing of starch-based material supplies has been detailed by Lam et al. 2002.

Water Absorption Capacity

Water absorption capacity (WAC) represents the ability of a substance to associate with water under a limited water condition and also indicates the ability of the starch to remain hydrated under specific time and temperature. WAC of rice starch used in this study was found to be $210.7 \pm 20.36\%$. Understanding the WAC of rice starch will lead to the interpretation of sample preparation that is rice starch concentration with water. Similar works were reported by Ashwar et al. (2017) for rice starch; the values were found to be between 150 and 280%.

Bulk Density, True Density, and Void Fraction

Bulk density depends on the particle size and initial moisture content of starches. The bulk density of rice starch was found to be 589.59 ± 34.74 kg/m^3. The high bulk density of starch suggests their suitability for use in food preparations. In contrast, low bulk density would be an advantage in the formulation of complementary foods. A similar study was conducted by Bhat and Riar (2019) who reported bulk density values of

Fig. 2 Particle size distribution of the rice starch
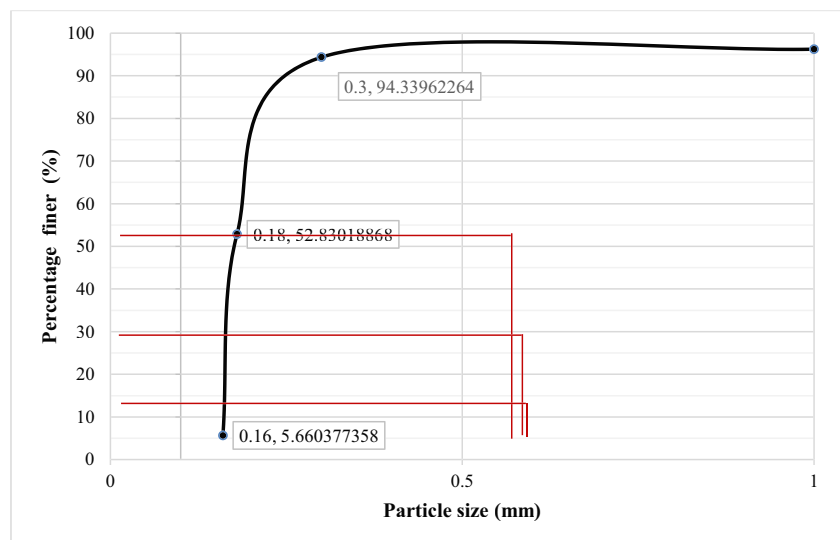
isolated starch of pigmented rice cultivars between 587 and 675 kg/m^3.

The true density value for the rice starch sample was found to be 1157.41 ± 80.18 kg/m^3. Material density is very important in assessing its printability; the higher density of the material, the higher force will be required to extrude the material. This can be achieved by adjusting motor speed (Lanaro et al. 2017).

The void fraction of the rice starch was calculated to be $57.22 \pm 14.69\%$. It explains the fraction of bulk volume occupied by pore space. The porosity of samples depends on factors including particle shape and particle size distribution (Wegrzyn et al. 2012). Samples with porosity have higher void space, which in turn increases absorption of water, thus improving its printability. Comparable range of values was obtained for the porosity of different rice varieties in a study conducted by Varnamkhasti et al. (2008).

Color Analysis

The addition of water to the rice starch decreased its lightness (Fig. 3). However, no significant difference was observed between the color values of rice starch and rice dough (material supply).

Pasting Behavior

The maximum viscosity during heating (peak viscosity), minimum viscosity after the peak, and final viscosity provide an indication of the pasting behavior of foods (Derossi et al. 2017). Holland et al. (2017) have reported the significance of viscosity in printing; generally, samples with higher viscosity show better printability. Rice starch showed peak viscosity at 2588 ± 378.14 cP (Table 1). The increase in viscosity is primarily due to granule swelling and can be correlated with the water binding capacity, explaining its influence on the final product. Hot paste viscosity is affected by amylose leaching, amylose lipid complex formation, and granule swelling (M. Li et al. 2018). The application of heat on starch granules in an aqueous solution will result in decreased crystalline zones. High pasting temperature (77.19 ± 4.27 °C) relates to resistance to swelling. During swelling, an increase in viscosity is evident, and leaching effects are prominent. Set back value depends on the molecular weight of amylose from granules and remains of gelatinized starch. Several studies have explained its relationship with cooking and eating properties (Singh et al. 2006; Rithesh et al. 2018).

Characteristics of 3D Printing Material Supply

Rice starch exhibits shear thinning behavior, thereby facilitating the extrusion behavior (Lille et al. 2018). Another significant use of starch in the food industry is that it is widely included as hydrocolloid, often used in food systems as a thickening agent. The starch thickening process involves the entanglement of conformally disordered polymer chains, which is otherwise referred to as polymer-solvent interaction. In this study, water was used as the binding agent for the material supply through better phase interactions (Yang et al. 2017; Yoo et al. 2005). Starch is naturally hydrophilic and can form hydrogen bonds upon oxidation or reduction. Owing to its hydrophilicity, starch exhibits strong inter-molecular interactions when it comes in contact with water molecules, forming a gel network, thereby aiding in the printability. The printability of rice starch is depended on the amount of water, the swelling pattern, the viscoelasticity of the material supply, and the interactions between the molecules.

Water Activity

The water activity of rice starch material supply was found to be 0.98 ± 0.01. These values were unaffected by the cold extrusion process. Nevertheless, it is important to adopt a suitable post-processing approach to improve the shelf-life of the 3D printed constructs.

Rheological Behavior

Steady Shear Rate The viscosity versus shear rate values for rice starch was fitted to the power law model (Eq. 4) ($R^2 = 0.94$). The material supply was prepared based on printing consistency requirements and exhibited shear thinning behavior with flow behavior index, $n < 1$ (Krishnaraj et al. 2019). The k value denoting the slope is the consistency index. Apparent viscosity of the rice starch dropped with the increase in shear rate and remained constant explaining the non-Newtonian pseudo-plastic behavior (Wang et al. 2018). This is significant as it relates to the ability of the material to extrude through the nozzle (Yang et al. 2018). The thixotropic behavior (Fig. 4a) of the sample is characteristic to cereal starches (Doublier 1981).

Foods with rheological stability can offer a wide range of printability (Kim et al. 2017). Kim et al. (2018) explained the significance of shear rate in 3D food printing. It is associated with the ability of the material to deform itself by its own weight and construction. Therefore, higher shear rates can be associated with the effects of extrusion speed, shape, and geometry of the 3D constructs. It is equally important that the printed object retains its structural stability during any subsequent stage of post-processing, handling, packaging, and storage.

Oscillatory Viscosity Understanding the viscoelastic behavior of the material supply can help in explaining the flow behavior of the material and its ability to retain its shape post-printing. Generally, materials with lesser viscosity flow easily through

Fig. 3 Comparison of the color analysis of the rice starch and material supply
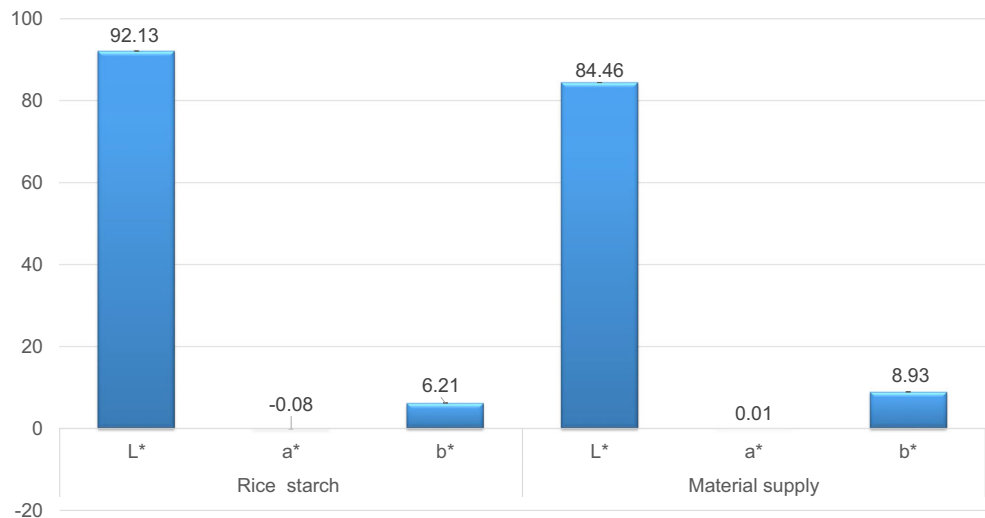
a small nozzle with high shear rates although the material has to recover high viscosity in order to hold back its dimensions after deposition (Lille et al. 2018). In this study, the viscoelastic properties of rice starch paste were measured by dynamic oscillatory viscosity. At higher temperatures, starch undergoes gelatinization, resulting in changes in material elasticity. Accordingly, peak storage modulus values were observed between 70 and 80 °C (Fig. 4b). An increase in the magnitude of both G' and G" can be attributed to starch swelling effects which in turn result in the formation of a closely packed gel network structure (Eliasson 1986).

The frequency dependence of G' and G" provides an essential idea about the structure of a material. A material that is independent of frequency over a time range forms a solid-like true gel system. On the other hand, a material with strong frequency dependence would exhibit structures with molecular entanglements that behave more like a liquid at a lesser frequency and solid at a higher frequency. In this study, frequency sweep was obtained over the range of 0.1 to 500 rad/s at 25 °C (Fig. 4c). Starch granules act as packing material in the dough and provide strong linkages that result in higher modulus (Sivaramakrishnan et al. 2004). Similar trends were observed

by Yoo et al. (2005) for rice starch dispersions. Higher storage modulus indicates that higher frequency would result in elastic gel–like starch structure, and at higher frequency, there is increased interior friction of the rice starch material (Wang et al. 2018). Loss tangent for the rice starch sample was found to tan $\delta < 1$, confirming that the material exhibits solid gel–like behavior with a strong network structure, which helps in printability and shape retention (Huang et al. 2019; Yang et al. 2017).

Printability of Rice Starch and Effect of Printing Variables

Printability explains the ability of material supply to undergo easy and uniform extrusion, while conserving its precision and accuracy during printing and retaining its stability after printing (Zhang et al. 2018). It is vital to understand both material compositions/structures and their implications on the printing process. The effect of printing variables such as printing speed, motor speed, and nozzle size on the printability of rice starch was studied.

Effect of Printing Speed

Print speed (arm speed of the delta printer) can be explained by considering the time-dependent distance covered by the nozzle during the printing process. At higher printing speed (up to 2400 mm/min), printing was improper, and the 3D construct had several structural defects. Accordingly, a maximum print speed of 2200 mm/min was fixed for this study. Higher speed resulted in lower thread quality, discontinuous threads, and poor overall product finishing. The best print quality was achieved with print speeds in the range of 1500 to 800 mm/min as evident from the print quality (Table 2). These explain uniform layer thickness, consistent appearance, and good stacking behavior (Liu et al. 2019c). Reducing

Table 1 Pasting properties of rice starch

Pasting properties	Values
Pasting temperature (°C)	77.19 ± 4.27
Peak viscosity (cP)	2588 ± 378.14
Hold viscosity (cP)	1059.99 ± 133.24
Final viscosity (cP)	3625.35 ± 259.87
Break down (cP)	1825.22 ± 78.34
Set back (cP)	1741.89 ± 231.6

*Pasting properties and rheology are mean ± SD of three experiments
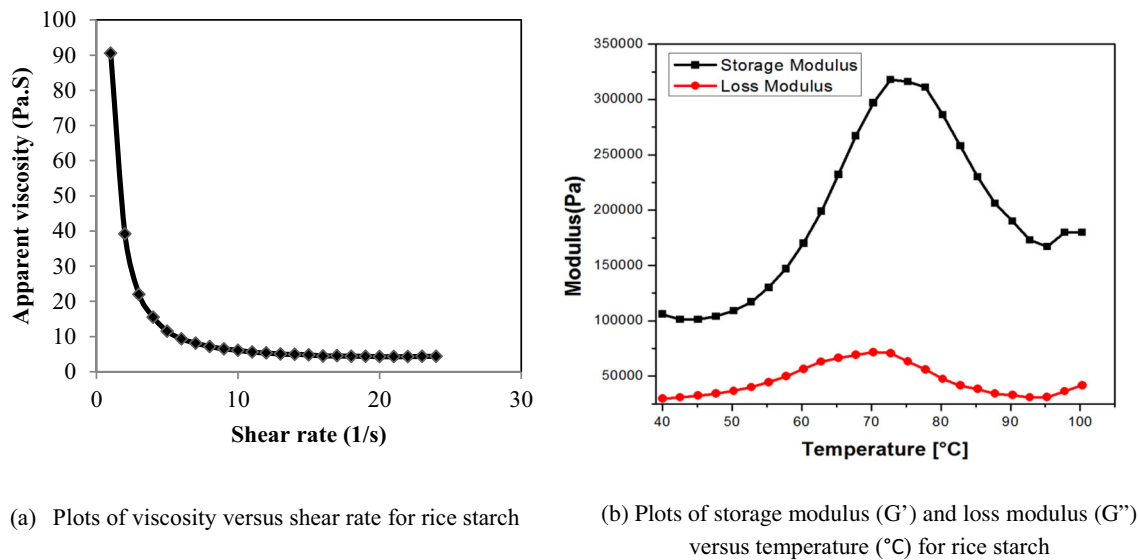
(a) Plots of viscosity versus shear rate for rice starch

(b) Plots of storage modulus (G') and loss modulus (G")
versus temperature (°C) for rice starch
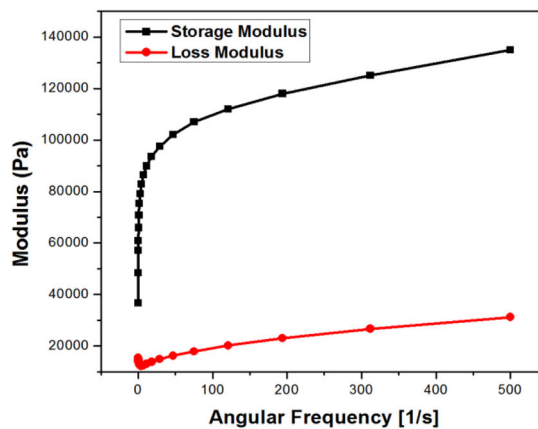
(c) Plots of storage modulus (G') and loss modulus (G") versus
angular frequency (1/s) for rice starch

Fig. 4 Apparent viscosity and dynamic oscillatory viscosity of the rice starch material supply. **a** Plots of viscosity versus shear rate for rice starch. **b** Plots of storage modulus (G') and loss modulus (G") versus temperature (°C) for rice starch. **c** Plots of storage modulus (G') and loss modulus (G") versus angular frequency (1/s) for rice starch
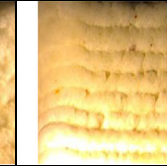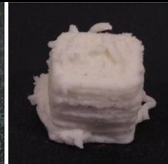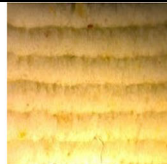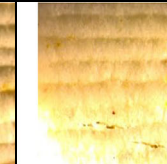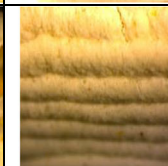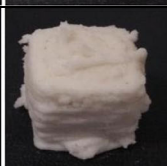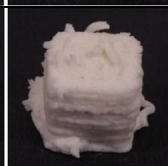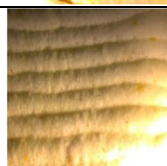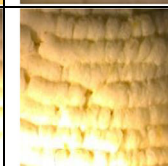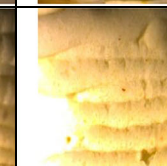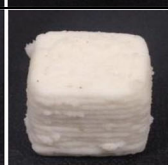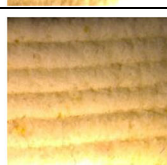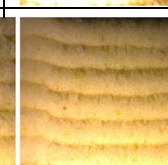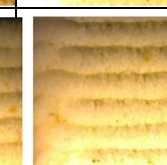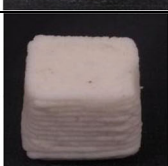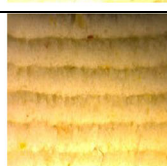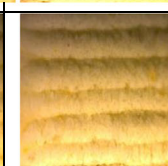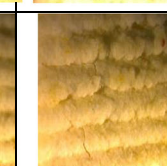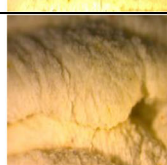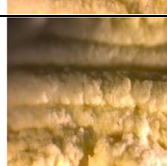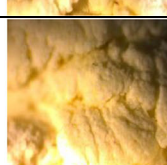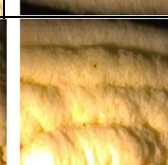
printing speed below 800 mm/min resulted in excessive printing time requirements apart from over extrusion of rice starch threads. Derossi et al. (2018) also explained that printing speed affects the distribution of pores in a product, also represented as infill porosity.

Effect of motor speed

Motor speed explains the extrusion of the material supply from the syringe and the auger drive that is attached to the motor. The extrusion rate is dependent on the motor speed; higher motor speeds result in higher extrusion rates. In this study, 100% speed (300 rpm) was avoided as it resulted in

back pressure. Keeping the motor speed between 120 and 180 rpm (40 and 60%) resulted in discontinuous threads. At 120 rpm (below 40%), the material could not be extruded. Motor speeds between 180 and 240 rpm (60 and 80%) were found to offer better printability. Similar studies were conducted by Derossi et al. (2018), and these researchers reported that higher motor speeds could result in irregular structures with high porosity, also affecting the characteristics of the end product. Proper prints of rice starch were obtained while maintaining reduced printing speeds (1500 to 800 mm/min) with motor speed between 240 and 180 rpm. The higher motor speed with higher printing speed resulted in improper printing. Similarly, the lower print speed with lower motor speed

Table 2 Effect of printing conditions on printability of rice starch

Nozzle size (mm)	Print speed (mm/min)	Printed rice starch cubes			Thread structure viewed under stereomicroscope at 20X		
		Motor speed (rpm)					
		240	180	120	240	180	120
1.2	2200						
	1500						
	800						
1.5	2200						
	1500						
	800						
1.7	2200						
	1500						
	800						

exhibited poor printability. Conversely, increased motor speed with lower print speed gave good printability.

Effect of Nozzle Size

Three different nozzle sizes (diameter) were selected for the study (1.2 mm, 1.5 mm, and 1.7 mm). Nozzle size influences the thread quality of the extruding material. Larger nozzle diameter (1.7 mm) extruded thick threads, and the printing precision was poor. While printing through 1.2-mm and 1.5-mm nozzles, the shape and geometry of the printed material could be better achieved. Therefore, optimized 1.2-mm and 1.5-mm nozzle diameters were preferred. Each nozzle size was evaluated for all three different motor speeds and three different printing speeds. The extrusion behavior of a material depends significantly on the type of material and the amount of force required for extrusion (Severini et al. 2016). The wet weight of the printed material notably increased from 1.4 to 3.7 g for varying nozzle sizes from 1.2 to 1.7 mm. Such a significant change in weight explains the relationship between printing variables and material metering in a printing process.

Effect of the Different Printing Process on Printing Rate

The effect of different printing variables on the printing rates was determined (Fig. 5). As expected, it was observed that the printing rate increased with increasing nozzle diameter. Maximum printing rate was observed with the 1.7-mm diameter nozzle at 800 mm/min and 240 rpm motor speed. In their study, Mantihal et al. (2017) compared the printing rates with

layer deposition in terms of diameter and concluded that the printing rate significantly affects sample dimensions.

Evaluation of 3D Printed Rice Starch Constructs

Microscopic Analysis

Variations in morphological characteristics were analyzed under a stereomicroscope (Table 2). In terms of visual appearance, nozzle diameter of 1.5 mm gave the best results. This was explained in terms of print infill, print deformity, thread breakages, and other structural aspects. These results are in agreement with results obtained by sensory evaluation. Constructs printed with low motor speed (120 rpm) and high printing speed (2200 mm/min) exhibited disturbed material flow and irregular extrusion, leading to cracks and fissures. Similar findings were reported by Le Tohic et al. (2017). Consistent structural dimensions can be obtained by optimizing motor speed. Besides motor speed, the nozzle size determines the thread quality. In other words, the uniform cylindrical structure of the printed thread depends on nozzle size among other variables.

Texture Analysis

Texture profile analysis (TPA) was conducted to evaluate the textural characteristics of the 3D printed constructs. TPA can explain the mechanical property and rheological stability of a printed material (Kim et al. 2017). The overall stability of a print can be confirmed with a TPA; poorly printed materials
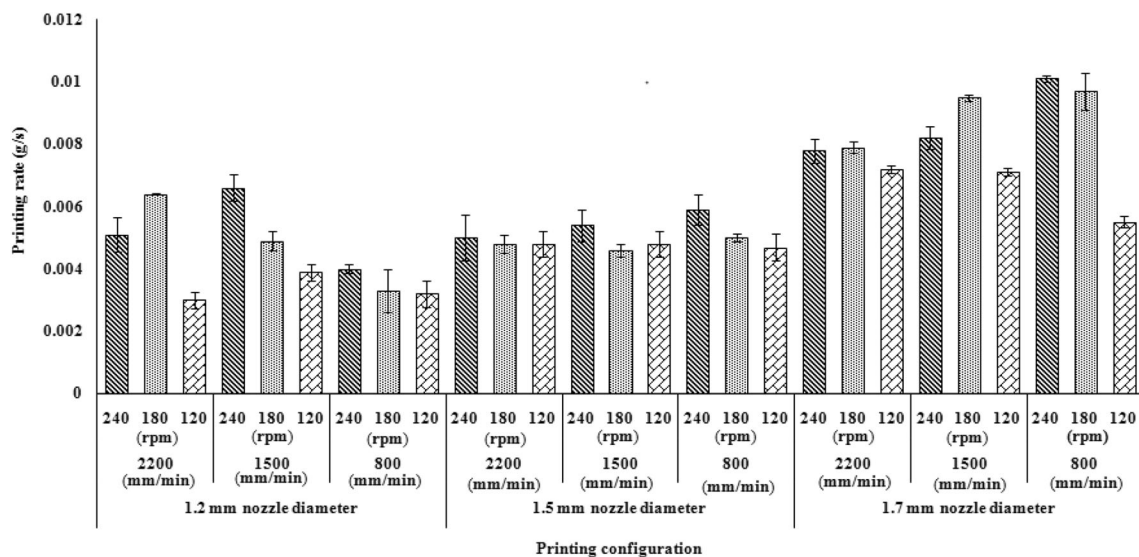
Result as observed for three print speeds (800,1500, and 2200 mm/min), three motor speeds (120, 1801 and 240 rpm), and three nozzle diameters (1.2, 1.5, and 1.7 mm).

Fig. 5 Effect of the different printing process variables on printing rate

exhibit weak textural properties. Moreover, determining the mechanical property of the printed material can aid in understanding the characteristic changes that occur in food during consumption and processing (Dankar et al. 2018). Samples printed with 1.2-mm diameter nozzle showed significant differences ($p < 0.05$) in hardness, fracturability, adhesiveness, and springiness (Table 3). Samples printed with 1.5-mm nozzle exhibited significant differences in hardness, fracturability, and adhesiveness. Hardness was found to be higher (4700.72 ± 426.88 g) for constructs printed using 1.7-mm nozzle with medium speed (1500 mm/min). The hardness of samples increased with compactness and thread thickness as established by the build volume of the prints. In a study conducted by Le Tohic et al. (2017) on different processed cheese, the researchers concluded that extrusion speeds did not affect product texture. In contrast, in this study, though most texture parameters were observed to have minimal changes, hardness

and fracturability of the 3D printed constructs were significantly affected by printing conditions.

Sensory Evaluation

The visual appearance of 3D printed rice starch constructs was assessed by sensory analysis. Observations were made by grading printed constructs based on a 9-point hedonic scale (Fig. 6). The grading criteria were selected in a manner that they consider the exterior design and appearance of the prints. Constructs printed using the 1.7-mm diameter nozzle showed poor overall acceptability. Over extrusion of the material supply was evident, and the 3D printed constructs had poor thread precision. Constructs printed with the 1.5-mm diameter nozzle with printing speeds ranging from 1500 to 800 mm/min and motor speeds between 240 and 180 rpm were better rated.

Table 3 Texture profile analysis of printed rice starch

Nozzle diameter (mm)	Print speed (mm/min)	Motor speed (%)	Hardness (g)	Fracturability (g)	Adhesiveness (g.s)	Springiness
1.2	2200	240	1845.52 ± 164.91[b]	− 516.79 ± 47.89[a]	− 113.76 ± 2.14[a]	0.09 ± 0.001[e]
		180	562.38 ± 121.74[a]	7764.51 ± 77.16[e]	− 85.51 ± 1.59[ab]	0.08 ± 0.001[d]
		120	462.33 ± 32.95[a]	− 440.76 ± 25.25[a]	− 67.97 ± 3.73[bc]	0.07 ± 0.001[c]
	1500	240	5210.20 ± 199.59[e]	− 531.72 ± 33.751[a]	− 75.53 ± 55.22[bc]	0.31 ± 0.004[f]
		180	4627.15 ± 331.27[d]	4022.03 ± 157.57[d]	− 6.46 ± 0.17[d]	0.05 ± 0.004[b]
		120	3100.83 ± 200.05[c]	696.71 ± 516.82[b]	− 2.73 ± 2.32[d]	0.04 ± 0.002[a]
	800	240	6397.11 ± 453.45[f]	− 519.68 ± 46.43[a]	− 44.17 ± 0.39[c]	0.06 ± 0.001[b]
		180	1559.61 ± 133.5[b]	2457.11 ± 311.72[c]	− 1.08 ± 0.06[d]	0.05 ± 0.001[b]
		120	7852.24 ± 41.71[g]	− 710.82 ± 47.87[a]	− 1.24 ± 0.03[d]	0.05 ± 0.001[b]
1.5	2200	240	12,649.52 ± 347.13[b]	− 434.95 ± 15.29[b]	− 92.47 ± 0.91[a]	0.08 ± 0.001[a]
		180	417.81 ± 1.39[a]	17,412.57 ± 100.11[f]	− 40.85 ± 0.94[d]	0.08 ± 0.001[a]
		120	250.49 ± 5.72[a]	− 652.43 ± 30.56[a]	− 77.81 ± 1.07[b]	0.08 ± 0.001[a]
	1500	240	21,702.19 ± 175.24[f]	− 384.42 ± 29.29[b]	− 40.71 ± 0.94[d]	0.09 ± 0.510[a]
		180	18,494.01 ± 323.92[e]	2844.70 ± 148.98[d]	− 24.57 ± 1.25[f]	0.16 ± 0.010[a]
		120	17,361.94 ± 404.81[d]	1043.45 ± 68.64[c]	− 23.09 ± 0.49[g]	0.18 ± 0.010[a]
	800	240	18,136.56 ± 134.50[e]	− 348.54 ± 24.30[b]	− 54.30 ± 1.8[c]	0.16 ± 0.010[a]
		180	26,181.45 ± 52.71[g]	3276.90 ± 79.44[e]	− 21.92 ± 0.90[g]	0.09 ± 0.0010[a]
		120	16,638.95 ± 334.18[c]	− 446.59 ± 10.14[b]	− 32.92 ± 0.16[e]	0.09 ± 0.513[a]
1.7	2200	240	18,297.95 ± 104.92[h]	− 548.50 ± 105.31[ab]	− 123.27 ± 10.70[b]	0.092 ± 0.001[b]
		180	73.6 ± 9.13[a]	7827.76 ± 284.59[e]	− 74.04 ± 12.27[d]	0.08 ± 0.0005[a]
		120	1156.51 ± 30.37[b]	− 345.17 ± 24.02[b]	− 172.07 ± 10.30[a]	0.07 ± 0.002[a]
	1500	240	5211.45 ± 69.01[f]	− 576.32 ± 61.37[ab]	− 108.08 ± 8.05[c]	0.034 ± 0.003[a]
		180	4700.72 ± 426.88[e]	3854.03 ± 100.84[d]	− 5.68 ± 0.922[f]	0.06 ± 0.001[a]
		120	3561.61 ± 339.48[d]	− 621.27 ± 53.40[ab]	− 4.86 ± 0.87[f]	0.06 ± 0.004[a]
	800	240	7071.65 ± 75.74[g]	− 523.12 ± 26.27[ab]	−41.63 ± 2.45[e]	0.05 ± 0.004[a]
		180	1526.05 ± 85.34[c]	2528.68 ± 346.97[c]	− 1.31 ± 0.15[f]	0.054 ± 0.005[a]
		120	1287.57 ± 192.71b[c]	− 662.86 ± 57.58[a]	− 1.58 ± 0.05[f]	0.06 ± 0.001[a]

*Texture profile values followed by the different alphabets in the same column are significantly different ($p < 0.05$) by Duncan's test

Code	Printing speed (mm/min)	Motor speed (rpm)
A	2200	240
B	2200	180
C	2200	120
D	1500	240
E	1500	180
F	1500	120
G	800	240
H	800	180
I	800	120
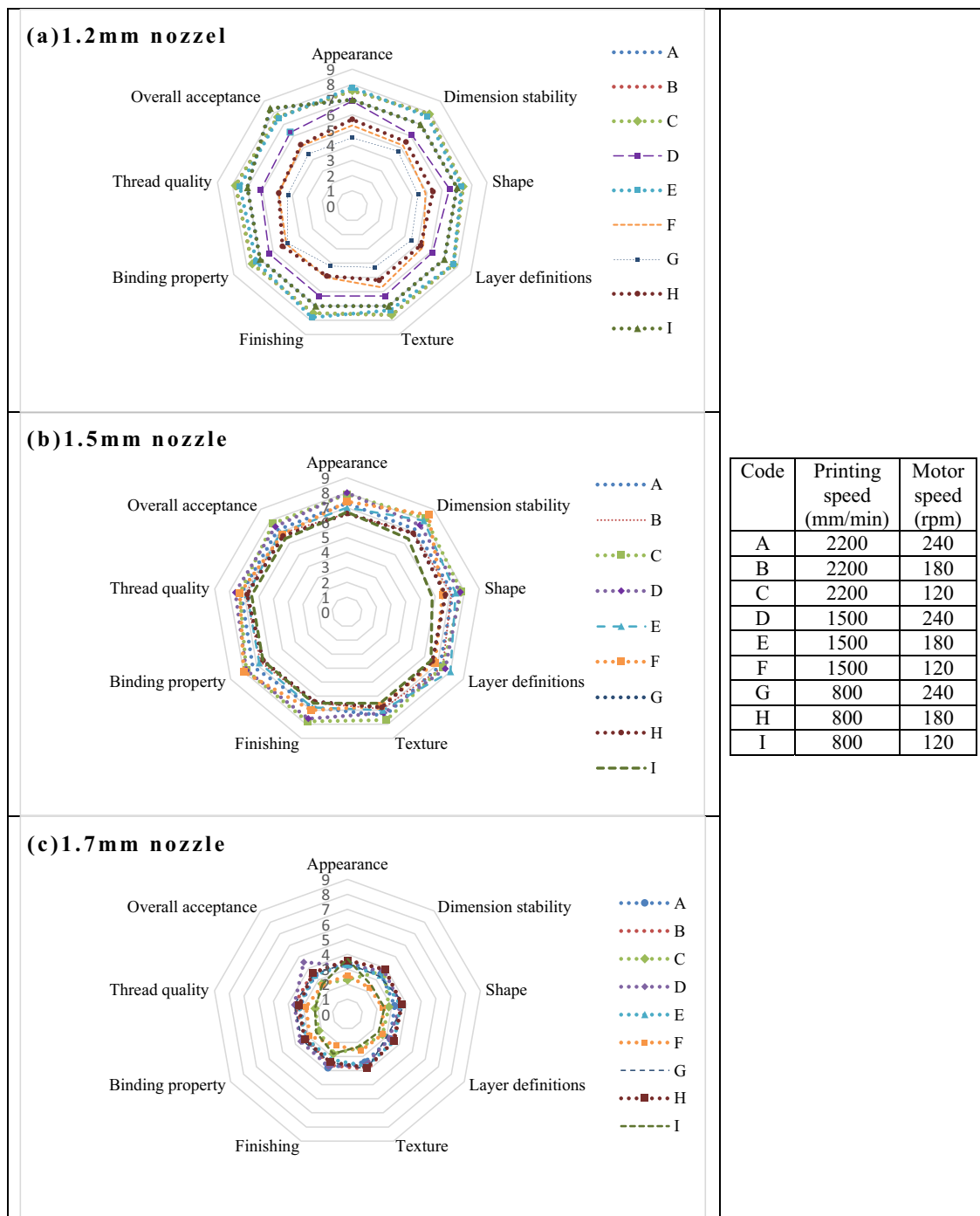
Fig. 6 Sensory evaluation of rice starch 3D printed using different printing conditions

Assessment of Printing Behavior with the Optimized Parameters

Based on results of sensory evaluation, an optimized set of printed samples were assessed for parameters such as shear rate (s^{-1}), velocity (m s^{-1}), and extrusion rate (cm^3 s^{-1}) (Table 4). Here, the extrusion rate relates to the volume of extruded material at a particular time. Similarly, shear rate, velocity, and extrusion rate also exhibited significant differences. This is because an increase in motor speed would result in an increase in the extrusion pressure, which in turn would result in extrusion of more material mass (Liu et al. 2019a). The cross-sectional area of the nozzle (nozzle diameter) is also responsible for these effects. Based on the results obtained, it is very evident that the extrusion rate majorly depends on motor speed.

Table 4 Assessment of printing behavior of the rice starch with the optimized nozzle (1.5 mm)

Parameters	Motor speed	
	180 rpm	240 rpm
Velocity (ms^{-1})	5.36 ± 0.40[a]	6.03 ± 1.32[b]
Shear rate (s^{-1})	27.13 ± 0.67[a]	30.53 ± 1.05[b]
Extrusion rate (cm^{3}s^{-1})	0.011 ± 0.001[a]	0.013 ± 0.002[b]

*Alphabets indicates significant difference at $p < 0.05$ between motor speeds

Conclusion

In this study, 3D printed constructs were developed from rice starch. The characteristics of the raw material (rice starch) and the material supply (rice dough) were studied. The effect of various printing conditions was evaluated, and printing using a 1.5-mm diameter nozzle at 1500 mm/min with a motor speed of 180 rpm was found to give the most acceptable constructs. Conclusions made by the sensory panelists were supplemented with a stereomicroscopic view of the 3D printed constructs. Printing using (and of) starch-based material supplies have huge research and commercial potential, and this study provides valuable information on the printability of rice starch, also providing insights for the development of rice starch–based 3D printed foods.

References

Alex, J., Dhanalakshmi, J., & Ambedkar, B. (2016). Experimental investigation on rice husk ash as cement replacement on concrete production. *Construction and Building Materials, 127*, 353–362.

Anukiruthika, T., Moses, J. A., & Anandharamakrishnan, C. (2020). 3D printing of egg yolk and white with rice flour blends. *Journal of Food Engineering, 109691*.

ASABE Standards. (2008). S319.4: Method of determining and expressing fineness of feed materials by sieving. St. Joseph, Mich.: ASABE.

Ashwar, B. A., Gani, A., Shah, A., & Masoodi, F. A. (2017). Physicochemical properties, in-vitro digestibility and structural elucidation of RS4 from rice starch. *International Journal of Biological Macromolecules, 105*(Pt 1), 471–477.

Asmeda, R., Noorlaila, A., & Norziah, M. H. (2016). Relationships of damaged starch granules and particle size distribution with pasting and thermal profiles of milled MR263 rice flour. *Food Chemistry, 191*, 45–51.

Bhat, F. M., & Riar, C. S. (2019). Effect of chemical composition, granule structure and crystalline form of pigmented rice starches on their functional characteristics. *Food Chemistry, 297*, 124984.

Cameron, D. K., Wang, Y.-J., & Moldenhauer, K. A. (2007). Comparison of starch physicochemical properties from medium-grain rice cultivars grown in California and Arkansas. *Starch-Stärke, 59*(12), 600–608.

Cao, C., Shen, M., Hu, J., Qi, J., Xie, P., & Zhou, Y. (2020). Comparative study on the structure-properties relationships of native and debranched rice starch. *CyTA-Journal of Food, 18*(1), 84–93.

Chen, H., Xie, F., Chen, L., & Zheng, B. (2019). Effect of rheological properties of potato, rice and corn starches on their hot-extrusion 3D printing behaviors. *Journal of Food Engineering, 244*, 150–158.

Chuanxing, F., Qi, W., Hui, L., Quancheng, Z., & Wang, M. (2018). Effects of pea protein on the properties of potato starch-based 3D printing materials. *International Journal of Food Engineering, 14*(3).

Daiuto, E., Cereda, M., Sarmento, S., & Vilpoux, O. (2005). Effects of extraction methods on yam (Dioscorea alata) starch characteristics. *Starch-Stärke, 57*(3–4), 153–160.

Dankar, I., Pujolà, M., El Omar, F., Sepulcre, F., & Haddarah, A. (2018). Impact of mechanical and microstructural properties of potato puree-food additive complexes on extrusion-based 3D printing. *Food and Bioprocess Technology, 11*(11), 2021–2031.

De La Hera, E., Gomez, M., & Rosell, C. M. (2013). Particle size distribution of rice flour affecting the starch enzymatic hydrolysis and hydration properties. *Carbohydrate Polymers, 98*(1), 421–427.

Derossi, A., Caporizzi, R., Azzollini, D., & Severini, C. (2017). Application of 3D printing for customized food. A case on the development of a fruit-based snack for children. *Journal of Food Engineering., 220*, 65–75. https://doi.org/10.1016/j.jfoodeng.2017.05.015.

Derossi, A., Caporizzi, R., Azzollini, D., & Severini, C. (2018). Application of 3D printing for customized food. A case on the development of a fruit-based snack for children. *Journal of Food Engineering, 220*, 65–75.

Dong, X., Huang, Y., Pan, Y., Wang, K., Prakash, S., & Zhu, B. (2019). Investigation of sweet potato starch as a structural enhancer for three-dimensional printing of Scomberomorus niphonius surimi. *Journal of Texture Studies., 50*(4), 316–324.

Doublier, J. L. (1981). Rheological studies on starch flow behaviour of wheat starch pastes. *Starch-Starke, 33*(12), 415–420.

Eliasson, A. C. (1986). Viscoelastic behaviour during the gelatinization of starch. I. Comparison of wheat, maize, potato and waxy-barley starches. *Journal of Texture Studies, 17*(3), 253–265.

Gayral, M., Fanuel, M., Rogniaux, H., & Dalgalarrondo, M. (2018). The spatiotemporal deposition of lysophosphatidylcholine within starch granules of maize endosperm and its relationships to the expression of genes involved in endoplasmic reticulum – amyloplast lipid trafficking and galactolipid synthesis, (April 2019). https://doi.org/10.1093/pcp/pcy198.

Ghazal, A. F., Zhang, M., & Liu, Z. (2019). Spontaneous color change of 3D printed healthy food product over time after printing as a novel application for 4D food printing. *Food and Bioprocess Technology, 12*(10), 1627–1645.

Godoi, F. C., Prakash, S., & Bhandari, B. R. (2016). 3d printing technologies applied for food design: status and prospects. *Journal of Food Engineering, 179*, 44–54.

Holland, S., Foster, T., Macnaughtan, W., & Tuck, C. (2017). Design and characterisation of food grade powders and inks for microstructure control using 3D printing. *Journal of Food Engineering., 220*, 12–19. https://doi.org/10.1016/j.jfoodeng.2017.06.008.

Horwitz, W., & LATIMER, G. W. (2000). *Official methods of analysis of AOAC international 17th edition* (pp. 43–44). Gaithersburg: AOAC International.

Huang, M., Zhang, M., & Bhandari, B. (2019). Assessing the 3D printing precision and texture properties of brown rice induced by infill levels and printing variables. *Food and Bioprocess Technology, 12*(7), 1185–1196.

Juliano, B. O. (1971). A simplified assay for milled rice amylose. *Cereal Science Today, 16*, 334–360.

Kim, H. W., Bae, H. J., & Park, H. J. (2017). Classification of the printability of selected food for 3D printing: development of an assessment method using hydrocolloids as. Journal of Food Engineering. Elsevier B.V. https://doi.org/10.1016/j.jfoodeng.2017.07.017.

Kim, H. W., Lee, J. H., Park, S. M., Lee, M. H., Lee, I. W., Doh, H. S., & Park, H. J. (2018). Effect of hydrocolloids on rheological properties and printability of vegetable inks for 3D food Printing. *Journal of food science, 83*(12), 2923–2932.

Keerthana, K., Anukiruthika, T., Moses, J. A., & Anandharamakrishnan, C. (2020). Development of fiber-enriched 3D printed snacks from alternative foods: A study on button mushroom. *Journal of Food Engineering.* https://doi.org/10.1016/j.jfoodeng.2020.110116.

Krishnaraj, P., Anukiruthika, T., Choudhary, P., Moses, J. A., & Anandharamakrishnan, C. (2019). 3D extrusion printing and post-processing of fibre-rich snack from indigenous composite flour. *Food and Bioprocess Technology*, 1–11.

Kumar, S., Anukiruthika, T., Dutta, S., Kashyap, A. V., Moses, J. A., & Anandharamakrishnan, C. (2020). Iron deficiency anemia: a comprehensive review on iron absorption, bioavailability and emerging food fortification approaches. *Trends in Food Science & Technology., 99*, 58–75. https://doi.org/10.1016/j.tifs.2020.02.021.

Lam, C. X. F., Mo, X. M., Teoh, S.-H., & Hutmacher, D. W. (2002). Scaffold development using 3D printing with a starch-based polymer. *Materials Science and Engineering: C, 20*(1–2), 49–56.

Lanaro, M., Forrestal, D. P., Scheurer, S., Slinger, D. J., Liao, S., Powell, S. K., & Woodruff, M. A. (2017). 3D printing complex chocolate objects: platform design, optimization and evaluation. *Journal of Food Engineering, 215*, 13–22.

Le Tohic, C., Sullivan, J. J. O., Drapala, K. P., Chartrin, V., Morrison, A. P., Kerry, J. P., & Kelly, A. L. (2017). Effect of 3D printing on the structure and textural properties of processed cheese. *Journal of Food Engineering.* https://doi.org/10.1016/j.jfoodeng.2017.02.003.

Li, J., & Nie, S. (2015). The functional and nutritional aspects of hydrocolloids in foods. *Food Hydrocolloids, 53*, 46–61. https://doi.org/10.1016/j.foodhyd.2015.01.035.

Li, M., Pernell, C., & Ferruzzi, M. G. (2018). Complexation with phenolic acids affect rheological properties and digestibility of potato starch and maize amylopectin. *Food Hydrocolloids, 77*, 843–852.

Lille, M., Nurmela, A., Nordlund, E., Metsä-Kortelainen, S., & Sozer, N. (2018). Applicability of protein and fiber-rich food materials in extrusion-based 3D printing. *Journal of Food Engineering, 220*, 20–27.

Liu, L., Meng, Y., Dai, X., Chen, K., & Zhu, Y. (2019a). 3D printing complex egg white protein objects: properties and optimization. *Food and Bioprocess Technology, 12*(2), 267–279.

Liu, Y., Zhang, W., Wang, K., Bao, Y., Mac Regenstein, J., & Zhou, P. (2019b). Fabrication of gel-like emulsions with whey protein isolate using microfluidization: rheological properties and 3D printing performance. *Food and Bioprocess Technology*, 1–13.

Liu, Y., Liang, X., Saeed, A., Lan, W., & Qin, W. (2019c). Properties of 3D printed dough and optimization of printing parameters. *Innovative food science & emerging technologies, 54*, 9–18.

Mantihal, S., Prakash, S., Godoi, F. C., & Bhandari, B. (2017). Optimization of chocolate 3D printing by correlating thermal and flow properties with 3D structure modeling. *Innovative Food Science & Emerging Technologies, 44*, 21–29.

Nachal, N., Moses, J. A., Karthik, P., & Anandharamakrishnan, C. (2019). Applications of 3D printing in food processing. *Food Engineering Reviews*, 1–19.

Nida, S., Anukiruthika, T., Moses, J. A. & Anandharamakrishnan, C. (2020). 3D printing of grinding and milling fractions of rice husk. *Waste and Biomass Valorization*, (123456789). https://doi.org/10.1007/s12649-020-01000-w.

Okaka, J. C., & Potter, N. N. (1977). Functional and storage properties of cowpea powder-wheat flour blends in breadmaking. *Journal of Food Science, 42*(3), 828–833.

Prabhakaran, B., & Moses, J. (2016). Pasting characteristics of raw rice flour obtained from various mill types. *Advances Ilife Sciences, 5*(5), 1605–1609.

Prabhuswamy, T., Tamilselvan, K., Michael, M. L., Moses, J. A., & Chinnasamy, A. (2019). Influence of different hydrocolloids on dispersion of sweet basil seeds (Ocimum basilicum) in fruit-flavoured beverages. *Croatian Journal of Food Science and Technology, 11*(1), 37–43. https://doi.org/10.17508/CJFST.2019.11.1.05.

Riaz, M., Akhter, M., Iqbal, M., Ali, S., Khan, R. A. R., Raza, M., … Shahzadi, N. (2018). Estimation of amylose, protein and moisture content stability of rice in multi locations.

Rithesh, B., Selvaraj, R., Doraiswamy, U., & Jeyaprakash, P. (2018). Characterization of physio-chemical properties of starch among traditional and commercial varieties of rice (Oryza sativa L .) using rapid visco analyser characterization of physio-chemical properties of starch among traditional and commercial varieties. *International Journal of Current Microbiology and Applied Sciencenternational Journal of Current Microbiology and Applied Science, 7*(October), 1490–1503. https://doi.org/10.20546/ijcmas.2018.710.167.

Román, L., Reguilón, M. P., & Gómez, M. (2018). Physicochemical characteristics of sauce model systems: influence of particle size and extruded flour source. *Journal of Food Engineering, 219*, 93–100.

Saikrishna, A., Dutta, S., Subramanian, V., Moses, J. A., & Anandharamakrishnan, C. (2018). Ageing of rice: a review. *Journal of Cereal Science, 81*, 161–170.

Samli, H. E., Nalbant, V., & Okur, A. A. (2013). Effects of microwave heating on some oil seeds nutrient contents and colour change. *Rivista italiana delle sostanze grasse, 90*(3), 183–188.

Severini, C., Derossi, A., & Azzollini, D. (2016). Variables affecting the printability of foods: preliminary tests on cereal-based products. *Innovative Food Science & Emerging Technologies, 38*, 281–291.

Shahzad, S. A., Hussain, S., Mohamed, A. A., Alamri, M. S., Akram, A., Qasem, A., & Osman, M. A. (2019). Pasting , thermal , textural and rheological properties of rice starch blended with 6 different hydrocolloid gums. *Pakistan Journal of Agricultural Sciences, 56*(3), 781–791. https://doi.org/10.21162/PAKJAS/19.6901.

Shen, Y., Zhang, N., Xu, Y., Huang, J., Wu, D., Shu, X., et al. (2019). Physicochemical properties of hydroxypropylated and cross-linked rice starches differential in amylose content. *International Journal of Biological Macromolecules, 128*, 775–781.

Singh, N., Kaur, L., Sandhu, K. S., Kaur, J., & Nishinari, K. (2006). Relationships between physicochemical, morphological, thermal, rheological properties of rice starches. *Food Hydrocolloids, 20*(4), 532–542.

Sivaramakrishnan, H. P., Senge, B., & Chattopadhyay, P. K. (2004). Rheological properties of rice dough for making rice bread. *Journal of Food Engineering, 62*(1), 37–45.

Sosulski, F., Garratt, M. D., & Slinkard, A. E. (1976). *Functional properties of ten legume flours*. Canadian Institute of Food Technology Journal.

Sun, J., Zhou, W., Huang, D., Fuh, J. Y. H., & Hong, G. S. (2015). An overview of 3D printing technologies for food fabrication. *Food and Bioprocess Technology, 8*(8), 1605–1615.

Tan, C., Toh, W. Y., Wong, G., & Lin, L. (2018). Extrusion-based 3D food printing–materials and machines.

Theagarajan, R., Malur Narayanaswamy, L., Dutta, S., Moses, J. A., & Chinnaswamy, A. (2019). Valorisation of grape pomace (cv. Muscat) for development of functional cookies. International Journal of Food Science & Technology.

Varnamkhasti, M. G., Mobli, H., Jafari, A., Keyhani, A. R., Soltanabadi, M. H., Rafiee, S., & Kheiralipour, K. (2008). Some physical

properties of rough rice (*Oryza sativa* L.) grain, *47*, 496–501. https://doi.org/10.1016/j.jcs.2007.05.014.

Wang, Y., Wang, L., Shephard, D., Wang, F., & Patindol, J. (2002). Properties and structures of flours and starches from whole , broken , and yellowed rice kernels in a model study properties and structures of flours and starches from whole , broken , and yellowed rice kernels in a model study. *Cereal Chemistry, 79*((3)(October 2015)), 383–386. https://doi.org/10.1094/CCHEM.2002.79.3.383.

Wang, L., Zhang, M., Bhandari, B., & Yang, C. (2018). Investigation on fish surimi gel as promising food material for 3D printing. *220*, 101–108. https://doi.org/10.1016/j.jfoodeng.2017.02.029.

Wegrzyn, T. F., Golding, M., & Archer, R. H. (2012). Food layered manufacture: a new process for constructing solid foods. *Trends in Food Science & Technology, 27*(2), 66–72. https://doi.org/10.1016/j.tifs.2012.04.006.

Yang, F., Zhang, M., Bhandari, B., & Liu, Y. (2017). Investigation on lemon juice gel as food material for 3D printing and optimization of printing parameters. *LWT - Food Science and Technology., 87*, 67–76. https://doi.org/10.1016/j.lwt.2017.08.054.

Yang, F., Zhang, M., Bhandari, B., & Liu, Y. (2018). Investigation on lemon juice gel as food material for 3D printing and optimization of printing parameters. *LWT, 87*, 67–76.

Yoo, D., Kim, C., & Yoo, B. (2005). Steady and dynamic shear rheology of rice starch-galactomannan mixtures, 310–318. https://doi.org/10.1002/star.200400390, 57, 7, 310, 318.

Zhang, L., Lou, Y., & Schutyser, M. A. I. (2018). 3D printing of cereal-based food structures containing probiotics. *Food Structure, 18*, 14–22.